Journal of Environmental Chemical Engineering 2 (2014) 927–934

Contents lists available at ScienceDirect

Journal of Environmental Chemical Engineering

journal homepage: www.elsevier.com/locate/jece

Influence of the iron content on the arsenic adsorption capacity of Fe/GAC adsorbents

Mirna E. Sigrist [a,*], Lucila Brusa [a], Horacio R. Beldomenico [a], Liza Dosso [b], Oksana M. Tsendra [c], Mónica B. González [b], Carlos L. Pieck [b], Carlos R. Vera [b]

[a] Programa de Investigación y Análisis de Residuos y Químicos Contaminantes de la Facultad de Ingeniería Química (UNL), Santiago del Estero 2654, 3000 Santa Fe, Argentina
[b] Instituto de Investigaciones en Catálisis y Petroquímica (FIQ-UNL, CONICET), Santiago del Estero 2654, 3000 Santa Fe, Argentina
[c] Chuiko Institute of Surface Chemistry, National Academy of Sciences, 17 General Naumov Street, Kiev 03164, Ukraine

ARTICLE INFO

Article history:
Received 29 August 2013
Accepted 20 February 2014

Keywords:
Arsenic adsorption
Groundwater
Fe/GAC
Arsenic remediation

ABSTRACT

Adsorbents of granular activated carbon doped with iron (Fe/GAC) were synthesized in the laboratory and their capacity for removal of arsenic species was measured by means of techniques of equilibrium adsorption and breakthrough curves. These data were obtained at room temperature and normal pH conditions. The materials were further characterized to determine their chemical composition and texture (specific surface, pore volume distribution). It was found that the adsorbents with 10%, 20% and 30% Fe had a great capacity for arsenic adsorption, showing uptake values of 2000–3500 μg of As per gram of Fe/GAC filter material. Doping with Fe increases the As adsorption capacity of granular activated carbon and the maximum capacity of adsorption is obtained with 10% Fe loading. Higher Fe contents decrease the capacity for arsenic removal. This was related to the decreased pore volume and pore size of the adsorbents with high Fe content. A decrease of surface accessibility due to pore plugging and a higher intraparticle diffusion resistance in the high loaded adsorbents would shift the point of bed breakthrough to lower values of eluted volume.

Introduction

Arsenic in groundwaters has received a lot of attention from environmental protection agencies, researchers and general public due to the noxious effects of arsenic on the human health. In many countries the arsenic level in water for human consumption is nowadays limited to a maximum of 50 $\mu g\ L^{-1}$ though in the most developed countries the limit has been further reduced to 10 $\mu g\ L^{-1}$ in recent years [1].

In comparison to other elements arsenic is particularly nocive to human health. Chronic exposure to arsenic by ingestion of contaminated water is known as HACRE (the Spanish acronym for Endemic Regional Chronic Hydro Arsenicism). The criteria for diagnosis of HACRE according to the WHO (World Health Organization) are: (i) a minimum exposure of 6 months to ingestion of contaminated water with more than 50 $\mu g\ L^{-1}$ of arsenic; (ii) appearance of skin eruptions typical of HACRE; (iii) non cancer related symptoms like weakness, chronic lung disease, portal fibrosis non cyrrotic of the liver, peripheral neuropathia, peripheral vasculopathia, feet and hands edema, etc.; (iv) skin cancer, Bowen illness, spinal cells carcinoma, spleen cells carcinoma; (v) high content of arsenic in the body: hair (>1 $mg\ kg^{-1}$), nails (>1.08 $mg\ kg^{-1}$), urine (>50 $\mu g\ kg^{-1}$) [2–4].

Many techniques of abatement of arsenic in contaminated water have been proposed [5]. However, the most used are only a few: flocculation, reverse osmosis and adsorption. Flocculation needs big facilities and trained personnel and consumes a relatively big amount of chemical per unit mass of removed arsenic. Reverse osmosis has a great efficiency and is especially recommended for the treatment of groundwaters with a high content of dissolved solids. However the cost of installation and maintenance of reverse osmosis plants is high and its efficiency for the removal of some As species is low. Adsorption is the preferred method for the point-of-use removal of arsenic, because of its operation simplicity and the relatively low cost of installation of the adsorption facilities. The use of adsorbents in industrial plants is not widespread, but the good efficiency for As removal and the low cost of implementation have resulted in the labeling of adsorption as "best available technique" for As removal by EPA, the environment protection agency of USA [6].

Adsorbents for arsenic abatement are invariably based on bulk or supported particles of oxides and hydroxides of transition

* Corresponding author. Tel.: +54 3424571161.
E-mail address: msigrist@fiq.unl.edu.ar (M.E. Sigrist).

http://dx.doi.org/10.1016/j.jece.2014.02.013
2213-3437/

Table 1
Capacity for arsenic adsorption of some bulk and supported adsorbents [6,7]. The average capacity was calculated from breakthrough curves obtained in RSSCT columns (feed concentration of 50 $\mu g\,L^{-1}$). The capacity is taken as the total amount of As adsorbed by the column (per unit volume) at the breakthrough point (outlet concentration of 50 $\mu g\,L^{-1}$).

Filter	Supplier	Type	Capacity ($mg_{As}\,L_{bed}^{-1}$)
E33	Severn Trent	Bulk	2300
ARM200	Engelhard	Bulk	550
GFH	Siemens	Bulk	2400
AAFS 50	Alcan	Supported	600
Metsorb G	Graver Hydroglobe	Bulk	1100
Adsorbia GTO	Dow Chemical	Bulk	800
Arxen X HIX	Purolite Solmetex	Supported	1800
Fe/GAC	–	Supported	1000–1500

metals like Fe, Zr, Ti and others. Some values of arsenic adsorption capacity are indicated in Table 1 for commercial and experimental filters. As it can be seen bulk adsorbents have a great adsorption capacity per unit volume of filter. However supported adsorbents are many times preferred because of their lower cost and their textural properties that are optimized for the use in packed beds [7].

Iron is particularly commonly used in applications of high processing capacity because of the low cost of fabrication of the adsorbent. The adsorption capacity of a Fe-based filter depends strongly on the amount of the surface species. For this reason industrial adsorbents are synthesized with techniques that maximize the specific surface area of the iron particles. The surface can be for example maximized by reducing the size of the iron oxide particles to the nanometer range [8]. Another strategy is that of supporting the active Fe species on other supports of high specific surface area, like alumina, activated carbon, resins, etc. [9–12].

Commercial adsorbents based on activated carbon supported metals have a convenient combination of properties: a relatively good capacity for arsenic adsorption, a low cost and the additional capacity for retaining chlorine, organic compounds, odorant compounds, heavy metals and bacteria [9]. Adsorbents of iron supported on activated carbon are particularly studied in this work. The focus is on assessing the impact of the iron content on the adsorption properties. Adsorbents with 10–30% Fe were thus synthesized and characterized in order to determine their capacity for abating arsenic in aqueous solution.

Only the adsorption of As(V) species was assessed. This choice was indicated by the similarity in As uptake by iron media, irrespective of the oxidation state of arsenic [13,14]. Moreover some authors reported that over Fe media As(III) is first oxidized to As(V) simultaneously with adsorption [15]. In addition, the almost exclusive dominance of As(V) species in groundwater from Santa Fe Province, Argentina, has been recently reported [16].

Experimental

Materials

Granular activated carbon was supplied by GAISA (Buenos Aires, Argentina). Iron trichloride ($FeCl_3$, 40% in water) was supplied by PPE Argentina SA. Activated carbons with nominal Fe contents of 10%, 20% and 30% were obtained by repeatedly impregnating the activated carbon granules by the incipient wetness method. The impregnating solution was the commercial $FeCl_3$ solution. In each impregnation step 20 g of activated carbon and 12 cm^3 of a solution of $FeCl_3$ (40% aqueous solution) were used. After each impregnation step the adsorbents were dried in a stove at 110 °C overnight. The Fe/GAC samples thus obtained were named as P-1 (10% Fe), P-2 (20% Fe) and P-3 (30% Fe). P-1 demanded one impregnation step, P-2 two impregnation steps and P-3 three impregnation steps.

Characterization

The Fe content of the adsorbents was determined by means of acid digestion followed by optical emission spectrometry. An amount of 0.03 g of the sample were burnt up to ashes at 800 °C for 5 h in air. The obtained ash was dissolved in 1:1 (the volume ratio between distilled water and 37 wt% hydrochloric acid) hydrochloric acid solution and further diluted to 100 ml. Then the iron content was obtained by analyzing the solution in an inductively coupled plasma optical emission spectrometer (Perkin Elmer, Optima 2100 DV) [17]. The textural properties were determined by nitrogen adsorption sortometry at 77 K in a Micromeritics Accusorb equipment. The specific surface area was determined by the BET method using point of the adsorption branch in the range $0.05 < (p/p_s) < 0.3$. The pore size distribution was determined using the BJH method and the desorption branch of the isotherm.

Adsorption isotherms

The arsenic adsorption isotherms were determined with the adsorbent in the powder form in order to eliminate diffusion constraints. The adsorbent granules were ground in an agata mortar to a grain size of 100–200 meshes. Four equilibrium points were measured for each adsorbent. For each point 100 ml of a solution of concentration 237–362 $\mu g_{As}\,L^{-1}$ and 9–24 mg of adsorbent were used. In each experience the powder and the solution were put in a flask and they were maintained with gentle stirring at room temperature for 7 days. Then the adsorbent was decanted and a sample of the solution was taken with a pipette. These samples were then analyzed to determine the As content by means of the arsine method [10]. The amount of arsenic in the solid was determined as the difference between the initial and final amounts of arsenic in solution. The solutions were prepared from a stock solution supplied by Merck (arsenic acid, H_3AsO_4, 1000 mg L^{-1}).

Regenerability of the adsorbents was tested by performing consecutive measurements of the adsorption isotherm with intermediate regeneration by washing the adsorbent with an alkali. The washing was performed by rinsing the adsorbent at room temperature with an amount of NaOH solution (0.1 mmol L^{-1}, pH = 10) equal to 10 times the volume of the solid sample. Then the sample was thoroughly washed with distilled water and dried at 110 °C in a stove before measuring the new adsorption isotherm.

Bed breakthrough curves

Dynamic bed breakthrough curves were measured by eluting a calibrated solution of As(V) (180 $\mu g\,L^{-1}$). The solution was pumped through a packed bed for many hours and the outlet concentration was measured by taking samples and analyzing them by atomic absorption and the arsine method. The adsorbent bed comprised 10 g of the Fe/GAC sample (crushed to a particle size of 35–80 meshes) supported by a quartz wool plug and located inside a stainless steel tube (AISI 304, 10 mm ID). A flowrate of 0.18 L h^{-1} was used and the pump was a Dosivac DEC 1070 one. The column height was 35 cm. For the column breakthrough experiments the adsorbent packing occupied a space of 22 cm^3 and had a height of 27 cm. The solution was pumped to the top of the column. The solution flowed downwards in the experiments. In this way there was no risk of bed expansion and channeling.

Results and discussion

Physicochemical characterization

The results of chemical composition confirmed the iron content of the adsorbents P-1, P-2 and P-3 with a maximum error of 4%. The results of the nitrogen sortometry tests are detailed in Table 2 and Fig. 1.

Last column in Table 2 shows the average Wheeler's radius as determined from the classical relation $r = 2V_g/S_g$. Other values of mean radius can be got as centers of the pore size distribution in Fig. 1. The values do not coincide simply because the distribution is skewed and has a tail in the wide pore region. In any case it can be deduced that the Fe addition decreases all texture parameters of the original activated carbon sample. While the decrease of the pore radius is approximately linear with the Fe content, the decrease of the specific surface area and the pore volume are not. Both decrease strongly as the Fe content is increased from zero to 10% and then progressively less at higher Fe contents.

It can be seen from the results of Table 2 and Fig. 1 that the pore radius is only slightly altered by the deposition of iron. This means that there is no preferential deposition of iron species in pores of a certain size. Particularly there is no preferential deposition or blocking of micropores.

Adsorption equilibrium and kinetics

The results of the adsorption isotherms plotted as a function of the percentage of Fe doping, are included in Fig. 2. The pH of the solution was not adjusted before the adsorption tests and the pH values measured corresponded to the equilibration of the original arsenite solution (pH = 3.8) and the solid. Measured pH values were about 3.3–3.4 at the end of the tests. P-2 and P-3 display very similar saturation values for arsenic adsorption (3380 and 3300 $\mu g_{As}\, g^{-1}$, respectively) indicating that values higher than 20% do not produce substantial improvements in the capacity of adsorption of the Fe/GAC adsorbent. This could be explained by considering that the maximum bidimensional packing of Fe active phase on the surface is got at 20% Fe content.

In the high dilution zone of the isotherms a linear relation, practically independent of the adsorbent used, can be got. The slope of the line is the Henry's constant for adsorption and it is equal to 90 ($L\, g^{-1}$). This value is higher than that reported by Sigrist et al. [11] for Fe/GAC adsorbents with 10% Fe, equal to 3.5 ($L\, g^{-1}$). This might indicate that the impregnation procedure in this work produces Fe active phase films of greater affinity for arsenic in solution.

The values of saturation capacity obtained for the adsorbents P-2 and P-3, 3300–3400 $\mu g_{As}\, g^{-1}$ are similar to the values of 3800 and 6460 $\mu g_{As}\, g^{-1}$ for Fe/GAC materials, found in an EPA report [12] and in the article by Solozhenkin et al. [18], respectively.

As indicated by Sigrist et al. [11] in the case of groundwaters used for human consumption the range of arsenic concentration most commonly found is 100–300 $\mu g As\, L^{-1}$. In the case of the adsorbents with low affinity for arsenic, even if they have a high saturation capacity the working range of the adsorption isotherm is the linear, high dilution, Henry's zone. It can be seen from Fig. 1 that the prepared Fe/GAC adsorbents can work in the saturation zone of the isotherm. This results in a more efficient use of the adsorbent and in a better performance of the filters for arsenic removal.

Table 2
Textural properties of the prepared adsorbents.

Sample	BET specific surface area BET, S_g ($m^2\, g^{-1}$)	Pore volume, V_g ($cm^3\, g^{-1}$)	Wheeler' pore radius, r_p (Å)
GAC	991.3	0.5735	11.6
P-1, 10% Fe	803.9	0.4484	11.1
P-2, 20% Fe	709.5	0.3798	10.7
P-3, 30% Fe	631.3	0.3263	10.3

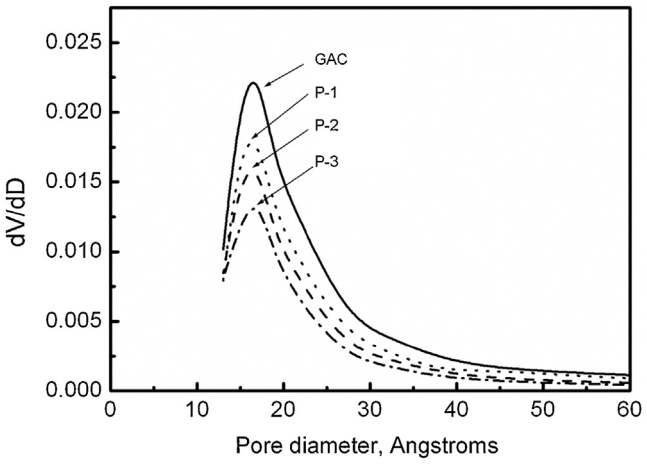

Fig. 1. Pore size distribution of the different samples.

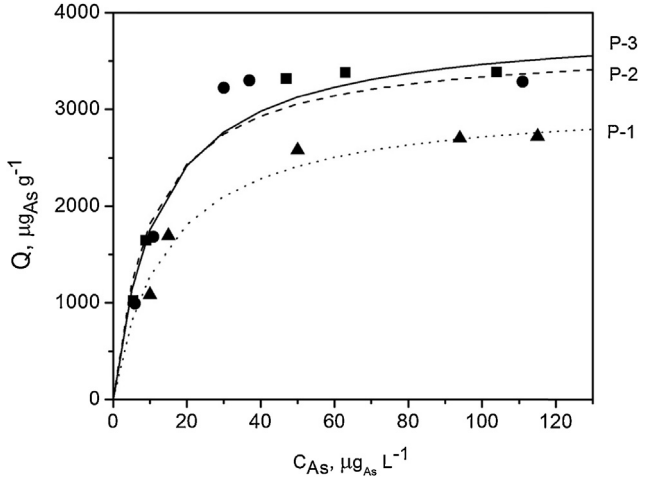

Fig. 2. Adsorption isotherms of As^V at 25 °C for the three Fe doped adsorbents. q, concentration of As in the solid; C_{As}, concentration of As in the liquid. Solid lines, Langmuir fitted model.

The data of Fig. 2 were fitted with the equations of Langmuir and Freundlich for adsorption (Eqs. (1) and (2)). In these equations Q_e is the equilibrium adsorption capacity of the adsorbate on the solid phase, Q_m is the saturation capacity (maximum capacity), C is the adsorbate concentration in the fluid phase, and L is Langmuir's constant for adsorption. A and n are the Freundlich's equation parameters.

$$Q_e = \frac{Q_m LC}{1 + LC} \tag{1}$$

$$Q_e = AC^{1/n} \tag{2}$$

The values of the parameters of the equations as long as the regression r^2 parameter are included in Table 3. It can be seen that fitting of the data with Langmuir's equation gives better results than fitting with Freundlich's equation. This is mainly the consequence of the saturation of the adsorbent surface at high values of arsenic concentration in the fluid phase.

Table 3
Fitting of equilibrium adsorption data to theoretical isotherm models.

Parameters		Units	P-1	P-2	P-3
Langmuir	R^2	–	0.9935	0.9770	0.9909
	K	$L\,\mu g_{As}^{-1}$	0.0699	0.0978	0.0821
	Q_m	$\mu g_{As}\,g_{ads}^{-1}$	3101.3	3678.9	3887.5
Freundlich	r^2	–	0.8425	0.7305	0.9038
	A	$\mu g_{As}\,g_{ads}^{-1}\,(\mu g_{As}\,L^{-1})^{-1/n}$	574.0	576.4	585. 6
	n	–	2.881	2.333	2.423

With respect to the kinetics of adsorption, no batch adsorption kinetic tests were performed and only breakthrough experimental data was available. In this sense some quantitative kinetic information can be obtained from the breakthrough curves of Fig. 3. Breakthrough curves however display information that is a convolution of many phenomena such as axial flow, intraparticle diffusion, film transfer and adsorption equilibrium. In this sense fitting is made easier if analytical expressions of the breakthrough curves were used that contain separate kinetic and equilibrium parameters. Analytical solutions exist in some cases of systems with simple adsorption isotherms [19]. These solutions include not only an adsorption model but also a model for movement along the packed bed, axial diffusion, film mass transfer, intraparticle diffusion, etc. Most theoretical solutions have been obtained for the cases of the square isotherm, the linear isotherm and the constant separation factor isotherm, coupled to models of linear concentration gradient in the film surrounding the adsorbent particle and Fickian diffusion inside the particles. Many of these solutions correspond to "constant pattern" approximations that reduce the solution to the movement of a stable mass front along the packed bed [19].

In our case the data of Fig. 3 can be conveniently modeled by a constant pattern solution based on the linear driving force (LDF) model for particle mass transfer [20] (Eq. (3)) and the constant separation factor isotherm (Eqs. (4)–(6)). As reported by Vermeulen and coworkers [21,22] the analytical solution for systems with Langmuir isotherms can be obtained by transforming the problem into one of "constant separation factor". These authors worked with pore diffusion and external mass transfer models, developing analytical and numerical solutions to the fixed bed adsorption kinetics under constant pattern and favorable isotherm conditions ($R < 1$ in Eq. (4)).

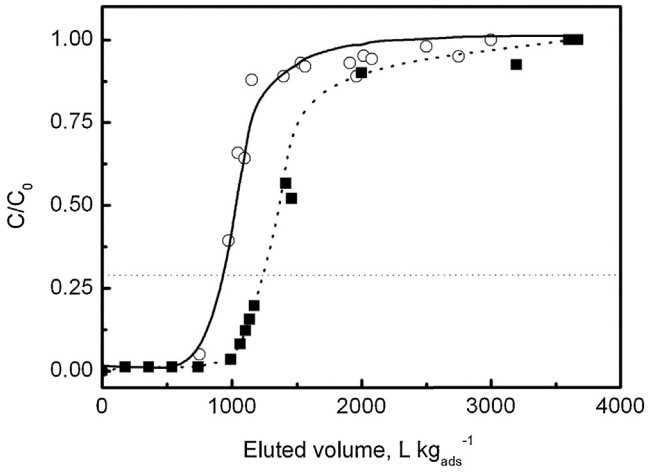

Fig. 3. Bed breakthrough curves for the P-1 (squares) and P-2 (circles) adsorbents. C^0 = 180 $\mu g_{As}\,L^{-1}$ arsenite in water, flowrate of 180 ml h^{-1}, adsorbent mass of 10 g. Breakthrough condition = 50 $\mu g_{As}\,L^{-1}$. Solid lines are the best fit curves of a model of constant separation factor isotherm and LDF kinetics.

$$\frac{dQ^*}{d\tau} = N(Q_e^* - Q^*) \tag{3}$$

$$R = \frac{C_e^*(1 - Q_e^*)}{Q_e^*(1 - C_e^*)} \tag{4}$$

$$C^* = \frac{C}{C^0} \tag{5}$$

$$Q^* = \frac{Q}{Q^0} \tag{6}$$

Vermeulen and coworkers [22] first presented a way of transforming Langmuir's equation in a way that resembles the constant separation factor isotherm by conveniently setting C^0 and Q^0 equal to the packed bed feed concentration and the equilibrium Q value corresponding to C^0 (Eq. (7)). Then they defined R (Eq. (8)) and rewrote the adsorption equation as in Eq. (9) after calculating Q/Q^0.

$$Q^0 = \frac{Q_m K C^0}{1 + K C^0} \tag{7}$$

$$R = \frac{1}{1 + K C^0} \tag{8}$$

$$Q_e^* = \frac{C^*}{R + (1 - R)C^*} \tag{9}$$

In the case of a favorable isotherm ($R < 1$) and particle mass transfer depicted by Eq. (3), the constant pattern solution is given by Eq. (10). In this equation the kinetic parameter, the time and the axial spatial coordinate have been written in adimensional form. Definitions of these adimensional quantities are given in equations (14–17). Λ is the partition ratio. The stoichiometric capacity of the bed for the solute is equal to Λ empty bed volumes of feed. L is bed length and z is the axial coordinate. v^{ref} is the interstitial velocity at the bed inlet, ε is the bed porosity and t is the time. ρ_b is the bed density.

$$\frac{1}{1 - R}\ln\left[\frac{1 - C^*}{C^{*R}}\right] + 1 = N(\zeta - \tau) \tag{10}$$

$$N = \frac{k_n \Lambda L}{\varepsilon v^{ref}} \tag{11}$$

$$\Lambda = \frac{\rho_b Q^0}{C^0} \tag{12}$$

$$\zeta = \frac{z}{L} \tag{13}$$

$$\tau = \frac{\varepsilon v^{ref} t}{L\Lambda} \tag{14}$$

Glueckauf and Coates [20] derived the linear driving force LDF approximation that relates the average adsorbate concentration inside the particle directly with the concentration in the fluid phase. By using the LDF approximation, the intraparticle mass balance equation is eliminated from the model and the solution to the global model of flow and adsorption is made easier. The LDF model combines the extraparticle and intraparticle diffusion and adsorption phenomena into one simple linear equation with one kinetic parameter, the overall k_n transfer parameter. The model correctly indicates that the driving force of the adsorption phenomenon is the difference between the actual adsorbent load and the equilibrium value.

Eq. (10) can be used to model the breakthrough curve by setting $\zeta = 1$ ($z = L$). A regression of this equation with the data of Fig. 3 was done using a Levenberg–Marquardt generalized least squares algorithm. The fitted values of k_n along with the values of some process variables are included in Table 4.

The obtained values of the overall kinetic LDF parameter ($k_n = 0.045–0.065$) are about twice the values reported by Zhang et al. [23] for the adsorption of arsenic over iron impregnated activated carbon felt ($k_n = 0.0232$). The fit of the theoretical solution chosen is reasonably good. The fitted values of the Λ parameter were however smaller than that calculated with Eq. (12) indicating that the full saturation of the adsorbent was not reached in the breakthrough experiments probably because of some part of the pore volume being plugged. This is evident when comparing the breakthrough curves of P-1 and P-2. The trace of P-2 is shifted to the left indicating that the bed is saturated more rapidly.

The adsorption isotherm results and the kinetic results can be compared with some data from literature, for other systems of similar adsorbents of microporous carbon impregnated with iron (see Table 5). This comparison indicates that the values of maximum adsorption capacity, Langmuir's constant and overall kinetic coefficient, are similar to those of similar adsorbents microporous carbon impregnated with iron. Only in the case of the results of reference [24] the adsorbent of iron supported over ordered mesoporous carbon (OMC) displays superior values of adsorption capacity and arsenic uptake kinetics.

Regenerability of the adsorbent

A simple procedure of regeneration was tried in order to test the reusability of the Fe/GAC adsorbent. Two P-1 samples were immersed in a concentrated arsenite solution (300 $\mu g_{As}\,L^{-1}$) and were allowed to reach equilibrium. After measuring the solution As concentration, the values of adsorbate concentration Q in the solid were calculated from the mass balance as 991 and 1082 $\mu g_{As}\,g^{-1}$ (residual equilibrium fluid phase concentration of 6 and 18 $\mu g_{As}\,L^{-1}$). The samples were then rinsed with 0.1 mmol L^{-1} NaOH solution (pH 10), thoroughly washed with deionized water and dried. Then they were subjected to another adsorption test that yielded values of Q of 866 and 975 $\mu g_{As}\,g^{-1}$ (residual equilibrium fluid phase concentration of 8 and 20 $\mu g_{As}\,L^{-1}$). This is about 80–90% the original capacity of the fresh adsorbent.

The Fe/GAC media can be therefore regenerated though extensive tests should be performed to clearly assess the number of times it can be used before it loses practical adsorption capacity. Tests for probing the leaching resistance of the surface Fe species should also be performed.

Table 4
Fitting of the data of the breakthrough curves with a constant pattern solution for constant separation factor isotherm ($R < 1$) and an LDF particle mass transfer model. Fitted parameters k_n and Λ.

Constant	Units	Value
WHSV, weight hourly space velocity	$g_{sol}\,h^{-1}\,g_{ads}$	18
C^0, feed As concentration	$\mu g_{As}\,L^{-1}$	180
Q^0, bed load capacity	$\mu g_{As}\,g_{ads}{}^{-1}$	2873
F_v, volumetric flowrate	$L\,h^{-1}$	0.18
v^{ref}, interstitial velocity	$cm\,h^{-1}$	572
ε, bed porosity	–	0.40
ρ_b, bed density	$g\,cm^{-3}$	0.38
R, separation factor, adsorbent P-1	–	0.0736
R, separation factor, adsorbent P-2	–	0.0538
k_n, overall kinetic constant for adsorption, P-1	h^{-1}	0.045
k_n, overall kinetic constant for adsorption, P-2	h^{-1}	0.065

Table 5
Compilation of some published results on the removal of arsenic from groundwater. The current results using Fe/GAC adsorbents are included for comparison. K, Langmuir constant for adsorption; Q_m, maximum adsorption capacity; k_n, pseudo first order global adsorption coefficient.

Material	K ($L\,\mu g_{As}{}^{-1}$)	Q_m ($\mu g_{As}\,g_{ads}{}^{-1}$)	k_n (h^{-1})	Reference
Fe/GAC	0.0699	2000–3000	0.045–0.065	This work
Fe/ACF	0.0480	4160	0.0232	23
Fe/GAC	0.00153–0.00265	199–2900	–	6
Fe/OMC	0.00629–0.00546	6400–7000	1.32	24

Effect of iron loading

An additional graph considering only the time values for the bed breakthrough (50 $\mu g\,L^{-1}$ condition) is included in Fig. 4, taken the Fe content as abscissa.

It seems against the common sense that the filter capacity is reduced at higher Fe contents. However it is possible that with 10% the maximum bidimensional density of Fe species is got. Higher loadings would only reduce the pore radius of the adsorbent and would increase the intraparticle mass transfer resistance. It is known the fact that the increase in the intraparticle resistance produces a deformation of the breakthrough curve, increasing the value of C/C^0 before the stoichiometric point and decreasing them after the stoichiometric point.

Goethite, an iron oxide commonly found in nature, has a cationic density of 5.8 atoms nm^{-2} in the ⟨100⟩ crystal plane, one of the most stable and abundant ones for this compound [25]. Considering a monolayer of one atom thickness with a goethite-like structure on activated carbon ($S_g = 991\ m^2\,g^{-1}$),

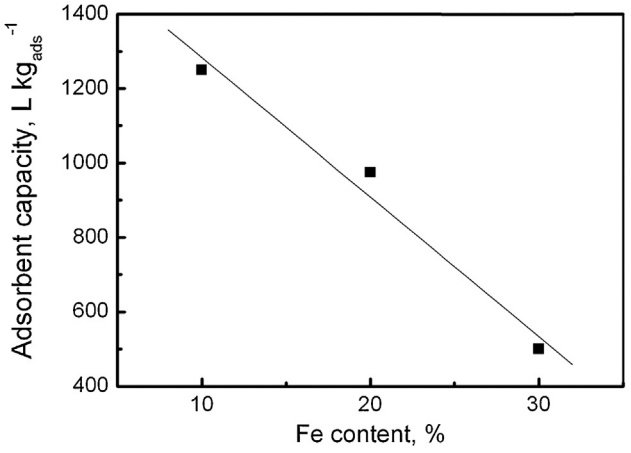

Fig. 4. Eluted volume ($L\,kg^{-1}$) in the point of bed breakthrough ($C_{outlet} = 50\ \mu g\,L^{-1}$) as a function of the Fe content of the adsorbent.

the iron content of the adsorbent would be 34% (see calculation below).

$$\text{Load} = \frac{991\ \text{m}^2\ \text{g}^{-1} 5.8\ \text{atoms}_{\text{Fe}}\ \text{nm}^{-2} 10^{18}\ \text{nm}^2\ \text{m}^{-2}\ 55845\ \text{gmol}^{-1}}{6.02\ 10^{23}\ \text{atoms}\ \text{mol}^{-1}}$$

$$\text{Fe}\,\% = \frac{\text{load}\,100}{1 + \text{load}}$$

If the maximum loading is 34% the early saturation of the surface could be alternatively explained by one of the following: (i) the bidimensional density of Fe in Fe/GAC is not that of goethite, but lower, i.e. 2 $\text{Fe}_{\text{atoms}}\ \text{nm}^{-2}$ because of the hydration of the Fe cation in solution; (ii) only the external layers of the activated carbon particles are effectively impregnated with Fe because of mass transfer problems; these problems being related to the small pore size of the carbon and the big size of the hydrated iron cation.

The elucidation of the mass transfer problem can only be done by inspecting the values of the respective sizes of the hydrated iron ions and the arsenite ion. Fig. 5 contains graphs of the structures of $FeCl_3(H_2O)_3$ and $(Fe(H_2O)_6)^{3+}$, the hydrated complexes of iron trichloride and its hydrolyzed counterpart. The geometry of these structures has been optimized using quantum-chemical methods. They were calculated with the density functional method B3LYP(6-311G(d) basis sets), because this level of theory has been an efficient method for predicting structures, frequencies and NMR chemical shifts of Fe^{3+} in aqueous solution [26]. It must be stressed that Fe^{3+} in aquo-chloro complexes can adopt different coordination geometries (e.g. tetrahedral, octahedral) but the coordination number is always six [27]. In this sense no bigger hydrated forms of Fe^{3+} should be expected. An inspection of the optimized structured indicates that the biggest dimension in the chloride or the hydroxide is the distance between opposite H atoms, 4.64–5.38 Å. These values agree with other published results [28] and are about one third of the mean diameter of the activated carbon material used. This is about one third of the mean diameter of the activated carbon material used.

In the case of the arsenic ions in solution, the pH stability ranges have been reported by Mondal et al. [29]. The stable As^V ions in quasi neutral pH conditions are $H_2AsO_4^{-1}$ and $HAsO_4^{-2}$.

The optimized structures of $H_2AsO_4^{-1}$ and $HAsO_4^{-2}$ in aqueous solution are drawn in Fig. 6. They were obtained with the quantum-chemical ab initio method Hartree–Fock/6-31G.

The biggest dimension in these complexes is about 3.6 Å. This is about one fifth the size of the pores of the adsorbents. From the point of view of the molecular size arsenic ions should be able to diffuse inside the Fe/GAC pore structure. Depending on the arsenite concentration however the mean free path between arsenite ions would be smaller than the distance between arsenite ions and the adsorbent pore walls. This would imply that pore diffusion could be controlled by Knudsen diffusion phenomena. Even in this case is most likely that the intraparticle diffusion is controlled by surface diffusion over the iron loaded surface. In this case low surface diffusivity values, in the order of $10^{-13}\ \text{m}^2\ \text{s}^{-1}$, which is orders of magnitude smaller than the molecular diffusivity of arsenic species (Sigrist et al. [11]).

In the movement inside the Fe/GAC pores free diffusion and adsorption is also influenced by the electrostatic forces of attraction/repulsion between the surface and the ions. It has been reported that the zero point of charge (ZPC) of Fe/GAC is 8.2–8.7 [30]. Hence at pH values of 6–8 the surface of Fe/GAC is positively charged and the adsorption of negatively charged complexes is favored by electrostatic attraction.

The same reasoning could be applied to the Fe complex during the impregnation procedure. These iron complexes are bigger than the arsenic ones and should diffuse very slowly into the activated carbon matrix. Given the short time used in the incipient wetness impregnation procedure is probable that the diffusion resistance would have favored a preferential loading of Fe on the outer layers of the carbon.

According to some authors the As(V) ion is adsorbed over the surface of oxides via a ligand exchange mechanism and exists in the form of an inner sphere surface complex [6]. The formation of mono dentate surface complexes has been considered to predominate over bi-dentate complexes at low values of surface coverage. At higher values of coverage by As(V), bidentate complexes are possible, but their formation seems to be slower [31].

The measured capacity for processing of As containing water, 1200–1300 L processed by kilogram of adsorbent, compares well

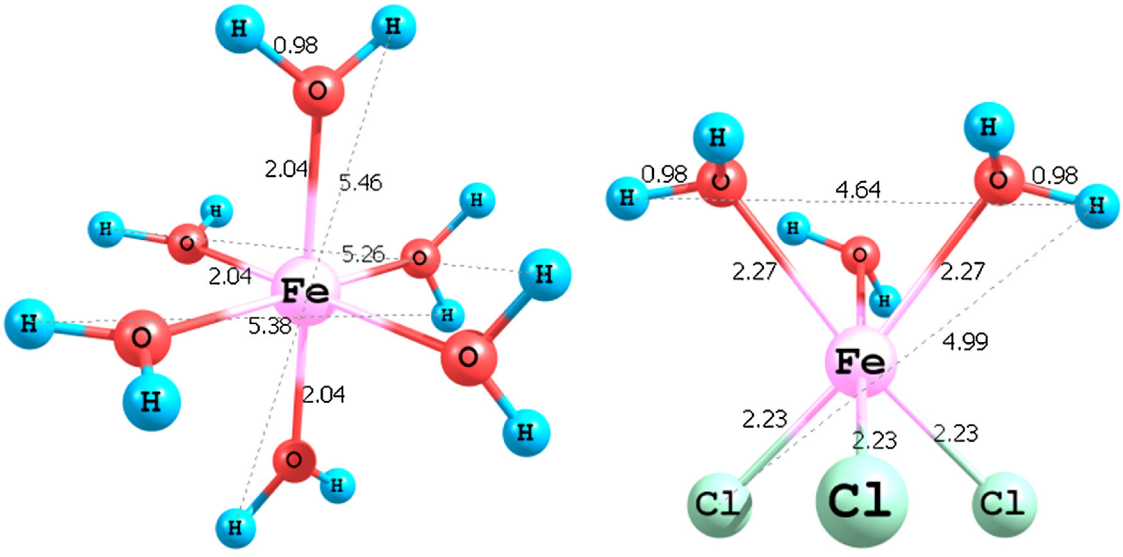

Fig. 5. Most stable iron species in solution in the conditions of impregnation, $(Fe(H_2O)_6)^{3+}$ (left) and $FeCl_3(H_2O)_3$. Interatomic distances as calculated by quantum-chemical methods.

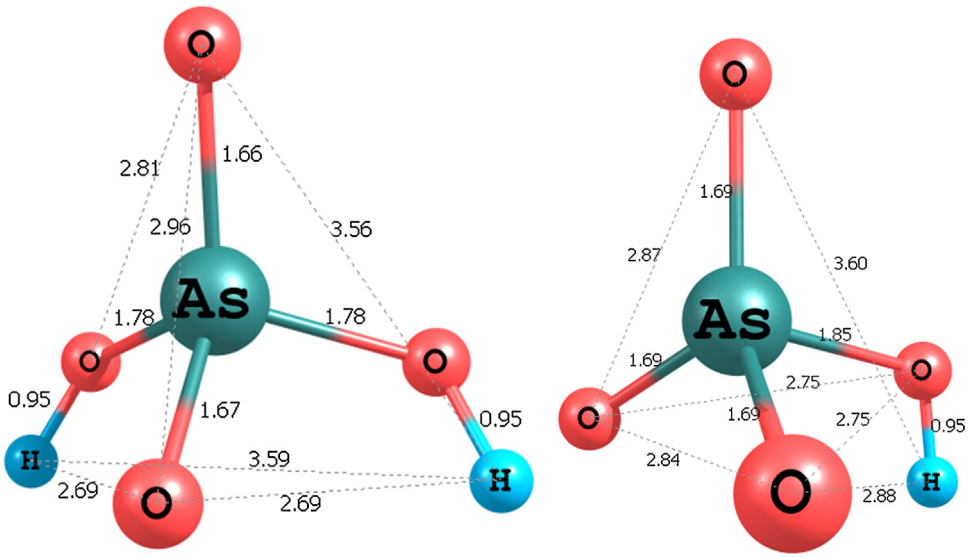

Fig. 6. Structures of $H_2AsO_4^{-1}$ (left) and $HAsO_4^{-2}$ (right) in aqueous solution.

with the value for other commercial adsorbents, as it can be seen in Table 1, moreover if the low cost of the Fe/GAC adsorbent is taken into account.

In the case of industrial size columns a 35–80 meshes particle size (as used in the experimental breakthrough test) is not convenient due to pressure drop limitations. A more convenient particle size could be 12–40 meshes.

Conclusions

The impregnation of iron over granular activated carbon produces adsorbents that are effective for the removal of arsenic from groundwaters. The maximum processing capacity for a breakthrough condition of 50 μg L^{-1}, is 1200–1300 L of water per kilogram of adsorbent. This value compares well with other values for commercial adsorbents of higher cost.

For three different values of Fe content, 10, 20 and 30%, it results that the best adsorbent is that of lower Fe content (10% Fe). This is thought to be mainly due to a saturation of the activated carbon particles by the combined effect of the big size of the hydrated Fe ions that yields a relatively low monolayer capacity and the slow diffusion of Fe, thus saturating preferentially the external layers of the carbon granules.

The decrease of the pore size of the carbon by Fe addition increases the intraparticle diffusion resistance thus provoking also a dynamic decrease of the adsorption capacity of the Fe/GAC filters.

References

[1] Environmental Health Criteria 224: arsenic compounds, 2nd ed., WHO, Geneva, 2001.
[2] T.S.Y. Choong, T.G. Chuah, Y. Robiah, F.L. Gregory Koay, I. Azni, Arsenic toxicity, health hazards and removal techniques from water: an overview, Desalination 217 (2007) 139–166.
[3] T.R. McClintock, Y. Chen, J. Bundschuh, J.T. Oliver, J. Navoni, V. Olmos, E. Villaamil Lepori, H. Ahsan, F. Parvez, Arsenic exposure in Latin America: biomarkers, risk assessments and related health effects, Sci. Total Environ. 429 (2012) 76–91.
[4] T. Yoshida, H. Yamauchi, G. Fan Sun, Chronic health effects in people exposed to arsenic via the drinking water: dose–response relationships in review, Toxicol. Appl. Pharmacol. 198 (2004) 243–252.
[5] M.I. Litter, M.E. Morgada, J. Bundschuh, Possible treatments for arsenic removal in Latin American waters for human consumption, Environ. Pollut. 158 (2010) 1105–1118.
[6] Z. Gu, J. Fang, B. Deng, Preparation and evaluation of GAC-based iron-containing adsorbents for arsenic removal, Environ. Sci. Technol. 39 (2005) 3833–3843.
[7] P.K. Westerhoff, T.M. Benn, A.S.C. Chen, L. Wang, L.J. Cumming, Assessing arsenic removal by metal (hydr)oxide adsorptive media using rapid small scale column tests, EPA/600/R-08/051, 2008.
[8] K.D. Hristovski, P.K. Westerhoff, T. Möllerc, P. Sylvester, Effect of synthesis conditions on nano-iron (hydr)oxide impregnated granulated activated carbon, Chem. Eng. J. 146 (2009) 237–243.
[9] S. Sato, K. Yoshihara, K. Moriyama, M. Machida, H. Tatsumoto, Influence of activated carbon surface acidity on adsorption of heavy metal ions and aromatics from aqueous solution, Appl. Surf. Sci. 20 (2007) 8554–8559.
[10] M. Sigrist, A. Albertengo, H. Beldoménico, M. Tudino, Determination of As(III) and total inorganic As in waters samples using an on-line solid phase extraction and flow injection hydride generation atomic absorption spectrometry, J. Hazard. Mater. 188 (2011) 311–318.
[11] M. Sigrist, H. Beldoménico, E.E. Tarifa, C.L. Pieck, C.R. Vera, Modelling diffusion and adsorption of As species in Fe/GAC adsorbent beds, J. Chem. Technol. Biotechnol. 86 (2011) 1256–1264.
[12] Arsenic Treatment Technology Evaluation Handbook for Small Systems EPA 816-R-03-014, 2003.
[13] T.D. Ciftçi, O. Yayayürük, E. Henden, Study of arsenic(III) and arsenic(V) removal from waters using ferric hydroxide supported on silica gel prepared at low pH, Environ. Technol. 32 (2011) 341–351.
[14] W. Chen, R. Parette, J. Zou, F.S. Cannon, B.A. Dempsey, Arsenic removal by iron-modified activated carbon, Water Res. 41 (2007) 1851–1858.
[15] P. Mondal, C.B. Majumder, B. Mohanty, Effects of adsorbent dose, its particle size and initial arsenic concentration on the removal of arsenic, iron and manganese from simulated ground water by Fe^{3+} impregnated activated carbon, J. Hazard. Mater. 150 (2008) 695–702.
[16] M. Sigrist, A. Albertengo, L. Brusa, H. Beldoménico, M. Tudino, Distribution of inorganic arsenic species in groundwater from Central-West Part of Santa Fe Province, Argentina, Appl. Geochem. 39 (2013) 43–48.
[17] H. Liu, G. Li, C. Hu, Selective ring C–H bonds activation of toluene over Fe/activated carbon catalyst, J. Mol. Catal. A: Chem. 377 (2013) 143–153.
[18] P.M. Solozhenkin, E.A. Deliyanni, V.N. Bakoyannakis, A.I. Zouboulis, K.A. Matis, Removal of As(V) ions from solution by akaganeite bgr-FeO(OH) nanocrystals, J. Mining Sci. 39 (2003) 287–296.
[19] M.D. LeVan, G. Carta, C.M. Yon, Adsorption and ion exchange fixed bed transitions, in: R.H. Perry, D.W. Green, J.O. Maloney (Eds.), Perry's Chemical Engineers' Handbook, 7th ed., Mc Graw-Hill, New York, 1997 (Chapter 16–33).
[20] E. Glueckauf, J.J. Coates, Theory of chromatography. Part IV. The influence of incomplete equilibrium on the front boundary of chromatograms and on the effectiveness of separation, J. Chem. Soc. (1947) 1315.
[21] T. Vermeulen, Adv. Chem. Eng. 2 (1958) 147.
[22] K.R. Hall, L.C. Eagleton, A. Acrivos, T. Vermeulen, Pore- and solid-diffusion kinetics in fixed-bed adsorption under constant-pattern conditions, Ind. Eng. Chem. Fundam. 5 (1966) 212–223.
[23] S. Zhang, X.-Y. Li, J.P. Chen, Preparation and evaluation of a magnetite-doped activated carbon fiber for enhanced arsenic removal, Carbon 48 (2010) 60–67.
[24] Z. Gu, B. Deng, J. Yang, Synthesis and evaluation of iron-containing ordered mesoporous carbon (FeOMC) for arsenic adsorption, Microporous Mesoporous Mater. 102 (2007) 265–273.
[25] V. Barrón, J. Torrent, Surface hydroxyl configuration of various crystal faces of hematite and goethite, J. Colloid Interface Sci. 177 (1996) 407–410.
[26] H. Ohtaki, T. Radnai, Structure and dynamics of hydrated ions, Chem. Rev. 93 (1993) 1157–1204.

[27] P.S. Hill, E.A. Schauble, A. Shahar, E. Tonui, E.D.E.D. Young, Experimental studies of equilibrium iron isotope fractionation in ferric aquo-chloro complexes, Geochim. Cosmochim. Acta 73 (8) (2009) 2366–2381.
[28] A. Stefánsson, K.H. Lemke, T.M. Seward, Iron(III) complexation in hydrothermal solutions – an experimental and theoretical study, in: Proceedings of the 15th International Conference on the Properties of Water and Steam, ICPWS, XV, vol. 15, September 8–11, Berlin, (2008), pp. 1–7.
[29] P. Mondal, C. Balomajumder, B. Mohanty, A laboratory study for the treatment of arsenic, iron, and manganese bearing ground water using Fe3+ impregnated activated carbon: effects of shaking time, pH and temperature, J. Hazard. Mater. 144 (2007) 420–426.
[30] B. Reed, R. Vaughan, As(III), As(V), Hg, and Pb removal by Fe-oxide impregnated activated carbon, J. Environ. Eng. 126 (9) (2000) 869–873.
[31] K.P. Raven, A. Jain, R.H. Loeppert, Arsenite and arsenate adsorption on ferrihydrite: kinetics, equilibrium and desorption envelopes, Environ. Sci. Technol. 32 (1998) 344–349.